This article has been accepted for publication in a future issue of this journal, but has not been fully edited. Content may change prior to final publication. Citation information: DOI 10.1109/TIA.2017.2784374, IEEE Transactions on Industry Applications

ISOGI-Q Based Control Algorithm for Single Stage Grid Tied SPV System

Bhim Singh, *Fellow, IEEE*, Priyank Shah, *Member, IEEE* and Ikhlaq Hussain, *Member, IEEE*

***Abstract*- This paper deals with a single stage solar photovoltaic (PV) array tied to a three phase grid by using an improved second order generalized integrator quadrature (ISOGI-Q) based control algorithm to improve power quality of the grid. The maximum point power tracking (MPPT) is achieved by using an incremental conductance method. The incremental conductance MPPT method is effective to extract crest power from a solar PV array as well as to control the DC bus voltage. The ISOGI-Q based control serves multi-functionalities such as load balancing, power factor correction, improved solar power penetration into a distribution network. Test results of ISOGI-Q based control algorithm, are found satisfactory for improved power quality in terms of load balancing, harmonics elimination and power factor correction very effectively under various dynamic conditions such as load unbalancing, variable solar insolation, distorted grid and imbalanced grid voltage conditions. DSTATCOM (Distributed Static Compensator) capabilities of PV based system are useful to supply the active power to the load and surplus power to the grid. The control algorithm is verified on a proposed topology and obtained responses are found satisfactory and total harmonic distortions (THDs) of source currents are observed within an IEEE-519 standard limit.**

Keywords- DSTATCOM, ISOGI-Q, MPPT, Power Quality, PV.

I. INTRODUCTION

Nowadays the use of solar power generation is booming because of increased research on SPV (Solar Photovoltaic), manufacturing technologies, rolling down price of SPV generation, new government policies and subsidy. However, conventional sources are main reasons for warming on the planet and having threat to the environment by using highly carbon intensive fuel like coal to keep energy economical [1-2]. Moreover, SPV based system is having advantaged of fast installation, eco-friendly and clean energy. Nowadays, photovoltaic (PV) system is used in residential, agriculture, telecommunication, healthcare services etc. Moreover, the power quality of the grid is degraded due to nonlinear loads like variable frequency drives (VFD), switch mode power supply (SMPS), arc furnace etc. in the distribution network at point of common coupling (PCC).

Manuscript received June 05, 2017; revised October 03, 2017; accepted November 22, 2017. This work was supported by the Department of Science and Technology, Government of India project under Grant RP02979. Paper no. 2017-PSEC-0512.

Bhim Singh and Priyank Shah are with the Department of Electrical Engineering, Indian Institute of Technology Delhi, New Delhi, India (e-mail: bhimsingh7nc@gmail.com and p4priyank1504@gmail.com).

Ikhlaq Hussain is with the Department of Electrical Engineering, Institute of Technology, University of Kashmir, Srinagar, J&K, India (e-mail: ikhlaqiitd@gmail.com).

Many techniques are introduced to implement PV model by Villalva et al. [3]. Many MPPT (Maximum Point Power Tracking) methods like differentiation technique, current compensation method, forced oscillation technique, look-up table method, perturb and observe method, load voltage maximization are available to extract maximum power point from SPV in the literature [4-5]. The reference voltage is obtained from MPPT and it is used further to maintain DC link voltage by proportional-integral (PI) controller. The power loss calculation for a single stage and a double stage grid-connected PV systems, is introduced by Wu et al. [6]. It is also mentioned that if the voltage range is properly chosen then a single stage has high efficiency, low cost and reducible size compared to a two stage grid connected solar PV based system. The double stage topology has lower efficiency compared to single stage topology due to considerable amount of losses in the boost converter. The advantages of single stage topology have been reported in the literature [7], are as follows,

- Single stage topology has high efficiency due to reduced losses.
- The elimination of boost converter reduces complexity, system size and cost.
- Solar PV array power utilization has been enhanced using single stage topology.

The voltage source converter (VSC) control algorithms are analyzed and proposed by many researchers. The d-q transformation based synchronous reference frame theory (SRFT) based control scheme has been analyzed by Tripathi et al. [8] for grid interfaced solar PV system for power quality improvement of distribution network. The control approach supports the voltage regulation and reactive power compensation. Still its dynamic performance is deteriorated due to presence of low pass filter in the procedure of tracking reference grid currents. The 2nd harmonic component is foremost in d-axis current under load unbalancing scenario. As a results, the steady-state performance is affected by setting high cut-off frequency. Therefore, it is consistently trade-off between steady-state and dynamic performances of the system. To eliminate this issues, Yazdani et. al. [9] have introduced the adaptive notch filtering (ANF) technique for three phase distribution network for power quality improvement of the distribution network. The ANF algorithm has zero DC offset rejection and lower harmonic filtering capabilities. Moreover, ideal phase and amplitude characteristics of the notch filter make it challenging to execute in the real-time scenario. Qasim et. al [10] have demonstrated the performance of

This article has been accepted for publication in a future issue of this journal, but has not been fully edited. Content may change prior to final publication. Citation information: DOI 10.1109/TIA.2017.2784374, IEEE Transactions on Industry Applications

multifunctional linear neuron and multi-layer neural network schemes to mitigate power quality issues such as harmonics mitigation, unity power factor, load balancing etc. for the distribution network. The neural network based control scheme has difficult to identify the proper learning.

The algorithms developed in the literature [11-13] for grid interfaced solar PV system focus on active power control strategies, which suffer from grid currents balancing feature and effectively harmonics mitigation. The various Lyapunov control schemes have been described for grid interfaced solar PV system in the literature [14-15] for power quality improvement of the distribution network along with extraction of maximum power from PV array. A model predictive control (MPC) scheme for grid interfaced converter has been analyzed in the literature [16]. However, it suffers from lack of grid currents balancing and has poor dynamic response. Various adaptive filters [17-19] based control schemes are also proposed to diminish power quality issues and improvement of solar power generation into the distribution network. The steady-state response of the least mean fourth (LMF) algorithm is not satisfactory due to having fourth order optimization technique. The mitigation of the noise at suitable frequency is not assured. The amplitude extraction capability of partial decoupled volterra filter depends upon the filter order. As filter order is increased, the computational burden and complexity of the algorithm are increased.

Many other algorithms such as adaptive filter generalized integrators [20-23] are described for power quality improvement of distribution network for various dynamic conditions. The second order generalized integrator (SOGI), second order generalized integrator-phase locked loop (SOGI-PLL) and second order generalized integrator frequency locked loop (SOGI-FLL) suffer from poor harmonic and DC offset rejection capabilities, which affects the system performance. The offset reduction generalized integrator has low pass filter in the path, which degrades the system performance. There is always trade-off between steady-state and dynamic performances of the system. To overcome the mentioned issues, an improved second order generalized integrator-quadrature (ISOGI-Q) based algorithm is proposed for three phase grid interfaced soar energy conversion system. The ISOGI-Q has good DC offset, lower order and higher order harmonic components rejection capability, which is demonstrated using frequency domain plot. The major contributions of presented work, lie in important characteristics of the control algorithm, which are as follows.

1. The fundamental component of load current in any phase, is extracted without sensing currents from remaining two phase, which makes reliable and phase independent.
2. To have fast dynamic performance during disturbed environmental conditions such as variable insolation, partial shading etc., PV feed-forward component is considered into the control scheme to make balanced and reduced oscillations in grid currents [24].
3. The frequency domain analysis demonstrates the effectiveness of proposed control scheme with conventional control algorithms.
4. The demand of reactive power at PCC is compensated by PV coupled VSC, which ensures unity power factor performance of the distribution network according to IEEE-519 standard [25].
5. The proposed control algorithm provides good performance even under weak grid conditions.
6. The presented ISOGI-Q based control algorithm has better filtering capabilities compared to conventional algorithm and it is reliable and flexible.

The proposed system consists of a single stage topology of a SPV based system having DSTATCOM (Distributed Static Compensator) capabilities interfaced to the grid to meet power quality improvement like power factor correction, load balancing. The ISOGI-Q based control algorithm has advantage of being less sensitive towards input DC offset and other harmonics and sub-harmonics. The control algorithm is very effective to estimate reference grid currents without loss of accuracy. To confirm viability of control algorithm, tests are performed on a developed hardware in the laboratory for various conditions like reactive power compensation, variable solar insolation, load unbalancing at load side network, distorted grid and imbalanced grid voltages.

II. Proposed System Configuration

The proposed system architecture contains a three phase grid, SPV array, ripple filter, DC link capacitor, VSC and nonlinear loads. Fig. 1 shows the proposed topology to validate the control algorithm. The proposed algorithm is implemented on a three phase grid tied single stage SPV based system. The proposed system parameters are designed as per procedure reported in [17-26].

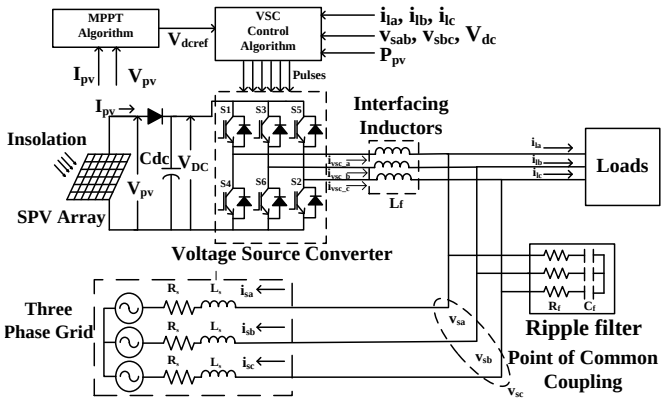

Fig. 1 The schematic diagram of proposed system topology

III. Control Algorithm

The ISOGI-Q based control algorithm is used to estimate quadrature component of fundamental load current. An incremental conductance MPPT method is utilized here to get maximum power point to operate SPV array at MPPT. This control algorithm is also used to mitigate power quality

This article has been accepted for publication in a future issue of this journal, but has not been fully edited. Content may change prior to final publication. Citation information: DOI 10.1109/TIA.2017.2784374, IEEE Transactions on Industry Applications

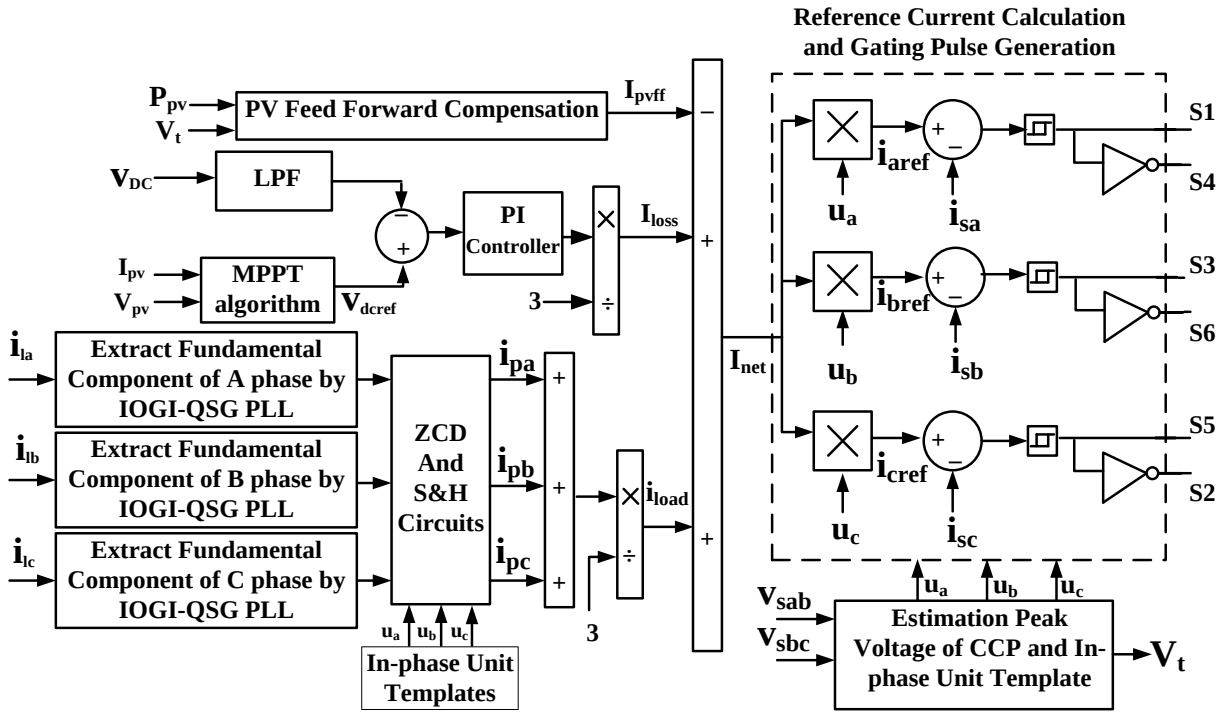

Fig. 2 Block diagram of control algorithm

problems. Fig. 2 depicts the overall structure of the control scheme.

A. MPPT Control

An incremental conductance MPPT method is used here to get operating point for a SPV array. The SPV voltage and current are sensed and used to estimate the difference between successive measurements of as following,

$$\frac{dP}{dV} = 0 \tag{1}$$

$$\frac{d(\mathrm{VI})}{dV} = I + V\frac{dI}{dV} = 0 \tag{2}$$

$$-\frac{I}{V} = \frac{dI}{dV} \tag{3}$$

In above equation, left hand side represents an incremental conductance and right hand side represent SPV array's instantaneous conductance. It is expressed under different operating condition as,

$$-\frac{I}{V} = \frac{dI}{dV}\left(\frac{dP}{dV} = 0\right) \tag{4}$$

$$-\frac{I}{V} > \frac{dI}{dV}\left(\frac{dP}{dV} < 0\right) \tag{5}$$

$$-\frac{I}{V} < \frac{dI}{dV}\left(\frac{dP}{dV} > 0\right) \tag{6}$$

Above equation is used to decide direction of perturbation to reach MPP point of SPV array. Whenever MPPT point is achieved then a change in current remains constant. Whenever, climate condition changes then a new MPP is tracked by an incremental conductance. This MPPT algorithm generates the reference DC link voltage for control of voltage source converter.

B. Switching Control of VSC

The switching control algorithm includes the estimation amplitude of terminal voltage at point of common coupling, estimation of in-phase unit templates, PV feed-forward term, loss component and reference currents estimation for three phase grid currents.

The amplitude of terminal voltage (V_t) at point of common coupling is evaluated by sensing line voltages (v_{sab} and v_{sbc}). From sensed two line voltages, phase voltages are obtained as [26],

$$\begin{bmatrix} v_{sa} \\ v_{sb} \\ v_{sc} \end{bmatrix} = \frac{1}{3}\begin{bmatrix} 2 & 1 & 0 \\ -1 & 1 & 0 \\ -1 & -2 & 0 \end{bmatrix}\begin{bmatrix} v_{sab} \\ v_{sbc} \\ 0 \end{bmatrix} \tag{7}$$

To reduce the influence of distortion and imbalances on the grid voltages on response of the system, a filtering method is utilized. The phase voltages are passed through the band pass filter to eliminate the harmonic distortions in the phase voltages. To eliminate imbalance and distortion in the grid voltages, the positive sequence of the phase voltages are obtained as [26],

$$\begin{bmatrix} v_{pa} \\ v_{pb} \\ v_{pc} \end{bmatrix} = \frac{1}{3}\begin{bmatrix} 1 & a^2 & a \\ a & 1 & a^2 \\ a^2 & a & 1 \end{bmatrix}\begin{bmatrix} v_{sa} \\ v_{sb} \\ v_{sc} \end{bmatrix} \tag{8}$$

where, $a = 1\angle 120$, $a^2 = 1\angle 240$.

This article has been accepted for publication in a future issue of this journal, but has not been fully edited. Content may change prior to final publication. Citation information: DOI 10.1109/TIA.2017.2784374, IEEE Transactions on Industry Applications

The amplitude of terminal voltage (V_t) is obtained as,

$$V_t = \sqrt{\frac{2}{3}\left(v_{pa}^2 + v_{pb}^2 + v_{pc}^2\right)} \tag{9}$$

The in-phase unit templates (u_a, u_b and u_c) are evaluated by using the amplitude of terminal voltage and phase voltages as,

$$u_a = \frac{v_{pa}}{V_t},\ u_b = \frac{v_{pb}}{V_t},\ u_c = \frac{v_{pc}}{V_t} \tag{10}$$

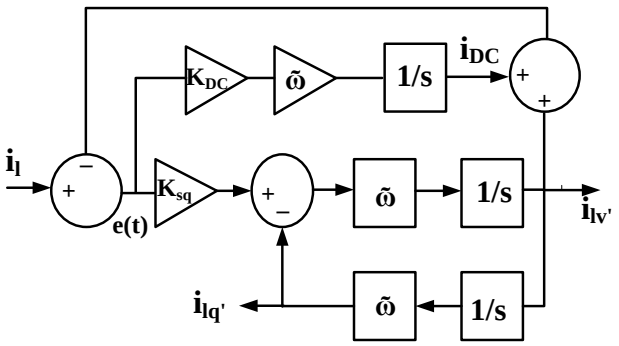

Fig. 3 Block Diagram of ISOGI-Q.

The ISOGI-Q based control method used here to extract the quadrature component of fundamental from load current, which is highly distorted due to nonlinear loads in the distribution network. Fig. 3 shows a structure of ISOGI-Q based control. The in-phase component ($i_{lv'}$) and quadrature component ($i_{lq'}$) of fundamental of load current are shown in Fig. 3. The transfer function of ISOGI-Q is given as,

$$\frac{i_{lv'}(s)}{i_l(s)} = \frac{k_{sq}\times\omega\times s^2}{\Delta(s)},\ \frac{i_{lqv'}(s)}{i_l(s)} = \frac{k_{sq}\times\omega^2\times s}{\Delta(s)} \tag{11}$$

$$\frac{i_{DC}(s)}{i(s)} = \frac{k_{DC}\times\omega\times(s^2+\omega^2)}{\Delta(s)} \tag{12}$$

where, $\Delta(S) = S^3 + (k_{sq} + k_{DC})\omega s^2 + \omega^2 s + k_{DC}\omega^3$, k_{sq} and k_{DC} are needed to tune with help of Routh-Hurwitz stability criterion. The parameter k_{DC} is opted based on $\Delta(s)$. All roots of $\Delta(s)$ must have equal real part.

Then k_{DC} must fulfill the condition as [17],

$$k_{DC}^3 + 3k_{sq}k_{DC}^2 + (3k_{sq}^2 + 9)k_{DC} + k_{sq}^2 - 4.5k_{sq} = 0 \tag{13}$$

The ISOGI-Q has high capacity to eliminate the DC offset from input signal by estimating it from error e(t) and added back to feed-back path. The amplitude of quadrature components for three phases (i_{pa}, i_{pb} and i_{pc}) are obtained by using unit templates, sample and hold logic respectively. From that amplitude, net weight of load component (I_{load}) is evaluated as,

$$I_{load} = \frac{i_{pa} + i_{pb} + i_{pc}}{3} \tag{14}$$

The PV feed-forward term is calculated by using SPV array power and it is estimated for a phase. Therefore, PV feed-forward (I_{pvff}) is evaluated as,

$$I_{PVff} = \frac{2P_{pv}}{3V_t} \tag{15}$$

The loss component is calculated by using reference DC link voltage obtained from MPPT and sensed VSC-DC link capacitor voltage. So loss component (I_{loss}) is evaluated as [26],

$$I_{loss} = \frac{1}{3}(V_{dcref} - V_{dc})(k_P + \frac{k_I}{s}) \tag{16}$$

The reference source currents are estimated by using in-phase templates (u_a, u_b and u_c) and net weight (I_{net}). The net weight (I_{net}) is obtained from load active current component (i_{ap}, i_{bp} and i_{cp}), SPV feed-forward term (I_{pvff}) and loss component (I_{loss}). The reference currents are calculated as,

$$I_{net} = I_{load} - I_{pvff} + I_{loss} \tag{17}$$

$$i_{aref} = u_a \times I_{net} \tag{18}$$

$$i_{bref} = u_b \times I_{net} \tag{19}$$

$$i_{cref} = u_c \times I_{net} \tag{20}$$

The error between source currents (i_{sa}, i_{sb} and i_{sc}) and estimated reference source currents (i_{aref}, i_{bref} and i_{cref}) are passed through the hysteresis controller and generate switching pulses for VSC.

III. Simulation Results

The proposed single stage grid interfaced solar PV system is modeled in MATLAB®/Simulink environment using Simscape toolbox [21]. The ISOGI-Q based control algorithm is proposed here to improve power penetration of solar PV array to distribution network, load balancing, harmonics mitigation, unity power factor correction etc. To demonstrate the system performance under dynamic condition, its behavior is analyzed under load unbalancing condition.

A. Dynamic Response of System under Unbalancing

Figs. 4(a-c) demonstrate the dynamic in the system under load unbalancing in phase 'a'. Fig. 4(a) illustrates DC link voltage, PV array current (I_{pv}), PV array power (P_{pv}), active and reactive grid power (P_s and Q_s) As unbalancing occurs in phase 'a', DC link voltage is maintained stable as shown in Fig. 4(a). The solar PV array power remains unaffected during load unbalancing, which are shown in Fig. 4(a). The load power is reduced due to unbalancing. Therefore, power flow in the grid is increased, which is depicted in Fig. 4(b). The reactive power flow in distribution network is zero which implies that distribution network operates at unity power factor operation as shown in Fig. 4(a). Fig. 4(b) shows the waveforms of grid voltages and currents (v_{sabc} and i_{sabc}), reference grid currents (i_{ref}), load current (i_{la}) and VSC current (i_{vsc}). As load unbalancing is occurred in phase 'a', grid currents are increased. The grid currents are successfully tracking reference grid currents as depicted in Fig. 4(b). The VSC currents are injected at PCC from solar PV array coupled VSC as depicted in Fig. 4(b). The salient intermediate signals such as in-phase and quadrature component of fundamental component ($i_{lv'}$, $i_{lq'}$), amplitude of fundamental component (I_{pa}), error (e), DC component (i_{DC}) are demonstrated in Fig. 4 (c). As load

This article has been accepted for publication in a future issue of this journal, but has not been fully edited. Content may change prior to final publication. Citation information: DOI 10.1109/TIA.2017.2784374, IEEE Transactions on Industry Applications

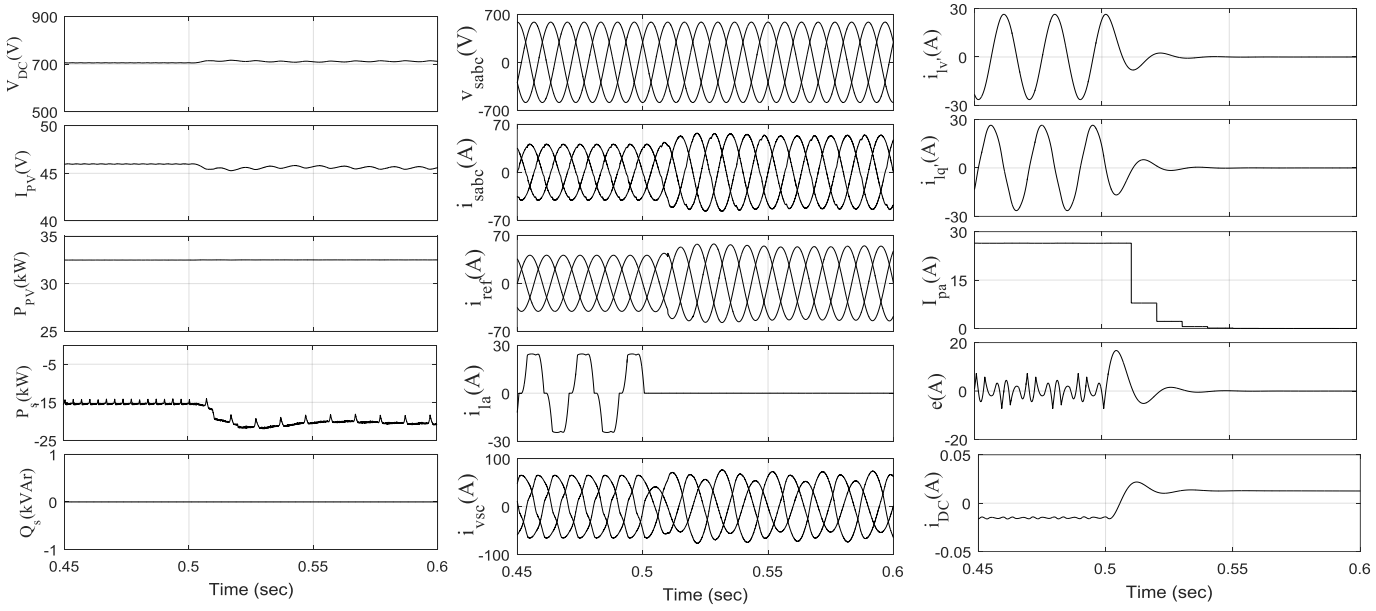

(a) (b) (c)

Fig. 4 Performance of the system under load unbalancing (a) V_{DC}, I_{pv}, P_{pv}, P_s, Q_s (b) v_{sabc}, i_{sabc}, i_{ref}, i_{la}, i_{vsc} (c) $i_{lv'}$, $i_{lq'}$, I_{pa}, e, i_{DC}

unbalancing occurs, in-phase and quadrature components of fundamental load current are decreased to zero as shown in Fig. 4(c).The amplitude of fundamental component of load current is also decreased to zero within couple of cycles. The dynamic of harmonic components and DC component in load current is shown in Fig. 4(c).

B. Comparative Performance of Proposed Control Algorithm

Fig.5 shows a comparative frequency domain performance of proposed ISOGI-Q and conventional SOGI-FLL. From Fig. 5, it is easy to analyze that the DC offset rejection capability of ISOGI-Q algorithm is higher than SOGI-FLL algorithm. The computational burden of ISOGI-Q is quite similar to conventional algorithms. The comparative behaviour of proposed ISOGI-Q and conventional algorithms are shown in Table-I. The LMF algorithm has no DC filtering capability, which leads to degrade the system performance. It is easy to

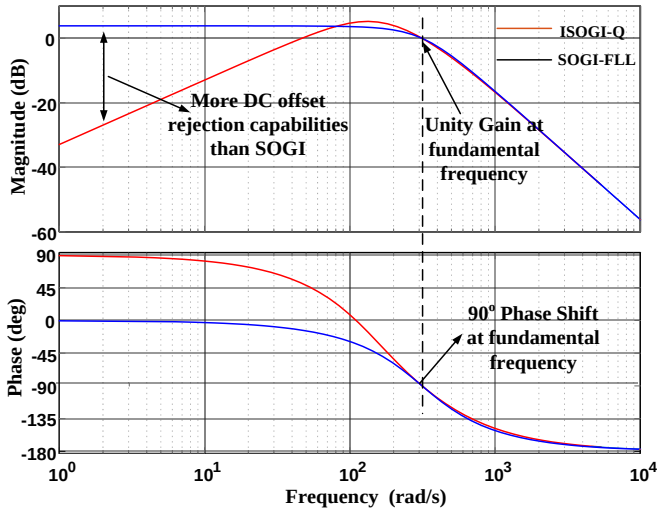

Fig. 5 Frequency domain analysis between ISOGI-Q and conventional SOGI-Q algorithm

TABLE I
COMPARISON BETWEEN VARIOUS ALGORITHMS

Parameters	ISOGI-Q (Proposed)	SOGI	SOGI-FLL	LMF
Filtering Type	Time domain based PLL	Time domain based PLL	Time domain based FLL	PLL-Less Adaptive Filter
Oscillation in Amplitude Estimation	0 A	0 A	0 A	6A
DC offset Filtering Capabilities	0.01053 (-45 dB)	0.1053 (-45 dB)	0.8607 (-3 dB)	NA
Degree/Order of Filter	3	2	2	4
Accuracy	Better	Good	Good	Poor
Phase shift of Fundamental Component	90º	0º	90º	NA
Complexity	Low	Low	Low	Low
Computational Time	2.29e-4s	2.13e-4s	3.65e-4s	3.94e-4s
Memory Required	Low	Medium	Medium	low

understand that proposed algorithm has many advantages such as low computational burden, high harmonics rejection capability, DC offset rejection over conventional control algorithms.

IV. EXPERIMENTAL RESULTS

This section shows the experimental results of proposed system topology to validate ISOGI-Q based control algorithm. The SPV simulator (AMTEK ETS600×17DPVF) is used as SPV array. The ISOGI-Q based control algorithm is implemented by a real time controller (dSPACE-1202). The voltages of PCC are sensed by voltage sensors (LV25-P) and source currents are sensed by current sensors (LA55-P). The

This article has been accepted for publication in a future issue of this journal, but has not been fully edited. Content may change prior to final publication. Citation information: DOI 10.1109/TIA.2017.2784374, IEEE Transactions on Industry Applications

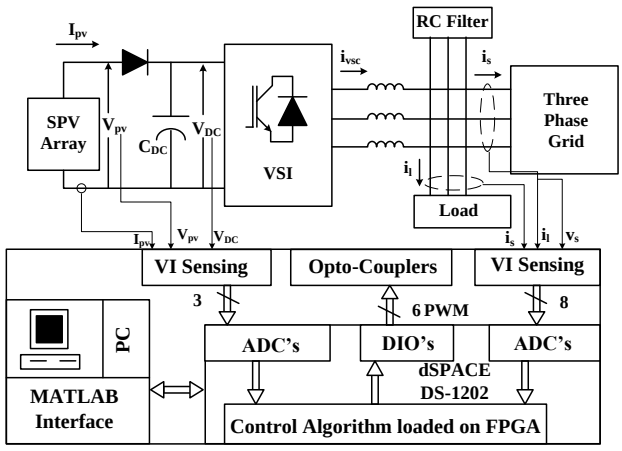

(a)

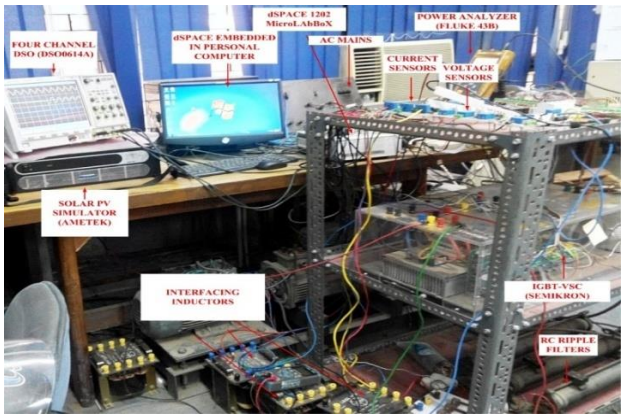

(b)

Fig. 6 (a) Block diagram of the experimental prototype (b) Photograph of the experimental prototype

dynamics of proposed system is observed by a digital scope oscilloscope (DSO) (AGILENT make DSO-7014A) and steady state response of proposed topology is observed by power analyzer (FLUKE make, 43B and YOKOGAWA make, WT-1800). The control algorithm is demonstrated here for various dynamic conditions such as load unbalancing, variable solar insolation, power factor correction, distorted grid voltages and imbalanced grid voltages. The schematic block diagram and photograph of the experimental system are shown in Figs. 6 (a-b).

A. Steady State Response of System Under Nonlinear Load

Fig. 7 shows the steady state response of the single stage grid connected SPV system. In this Fig. 7, the waveforms of grid voltage (v_{sab}), grid current (i_{sa}), load current (i_{la}) and VSC current (i_{vsc_a}) are shown. Figs. 7(a-c) show the waveforms of grid voltage (v_{sab}) and grid current (i_{sa}), v_{sab} and load current (i_{la}), v_{sab} and VSC current (i_{vsc_a}) respectively. Figs. 7(d-f) show that SPV array power not only supplies power to the load however, it also supplies to the grid by improving power quality of the grid. Fig. 7 (g) shows that THD of load current as 27.1%. Fig. 7 (h) shows that THD of grid current (i_{sa}) as 3.6%. It follows IEEE-519 standard [25].

B. Steady State Performance of the System Under Linear Load

Figs. 8(a-f) depict the steady state performance of the proposed system under a linear load. Figs. 8(a-c) show v_{sab} with

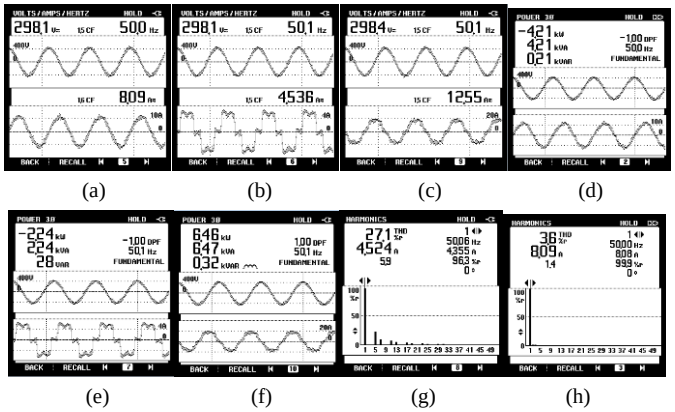

(a) (b) (c) (d) (e) (f) (g) (h)

Fig. 7 Steady state performance under nonlinear loads (a) v_{sab} with i_{sa} (b) v_{sab} with i_{la} (c) v_{sab} with $i_{vsc\text{-}a}$ (d-f) grid, load and SPV-VSC power (g) THD of i_{la} (h) THD of i_{la}

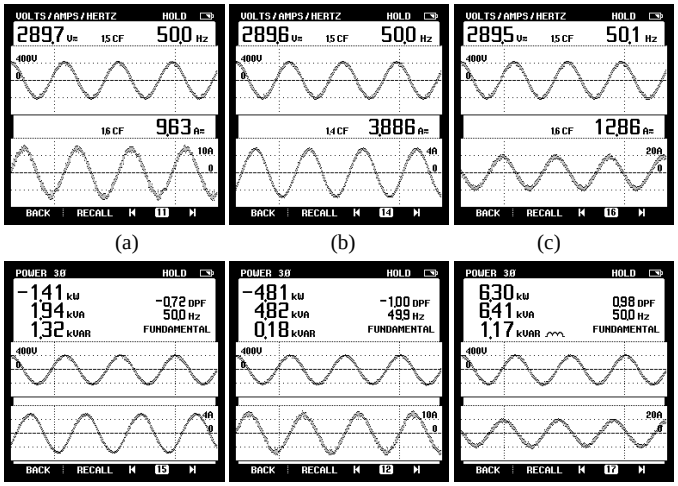

(a) (b) (c) (d) (e) (f)

Fig. 8 Steady state behaviour of system under linear load (a) v_{sab} and i_{sa}(b) v_{sab} and i_{la}(c) v_{sab} and i_{vsc_a} (d) load power (e) grid power (f) SPV-VSC power

i_{sa}, i_{la}, and i_{vsc_a} respectively. Fig. 8(d) shows load power (1.94kVA) at poor power factor (PF=0.72). Fig 8(e) depicts the improvement of power factor of the distribution network to unity. Moreover, the reactive power compensation is achieved by SPV coupled VSC based topology. Fig. 8(f) shows SPV coupled VSC power (P_{vsc}). The SPV array coupled VSC based topology supplies an active power and the reactive power to the distribution network and the load.

C. Dynamic Response of System under Distorted Grid Condition

Figs. 9(a-d) illustrate the dynamics of the system under weak grid condition. Figs. 9(a-b) show the behaviour of the system parameters before switching on VSC. Fig. 9 (a) shows the waveforms of the grid voltages and grid currents under nonlinear load. Due to weak grid condition, the grid voltages have high THDs due to highly nonlinear load connected at PCC. The THDs of grid voltages and currents are higher than IEEE-519 standard limits as depicted in Fig. 9 (b). The power flow in the grid is same as the load power, as depicted in Fig. 9 (b). When PV array coupled VSC is connected to the PCC, the solar power generation supplies power to the local loads and additional power to the grid. Therefore, corresponding increased power flow in the grid is depicted in Fig. 9 (c). The

This article has been accepted for publication in a future issue of this journal, but has not been fully edited. Content may change prior to final publication. Citation information: DOI 10.1109/TIA.2017.2784374, IEEE Transactions on Industry Applications

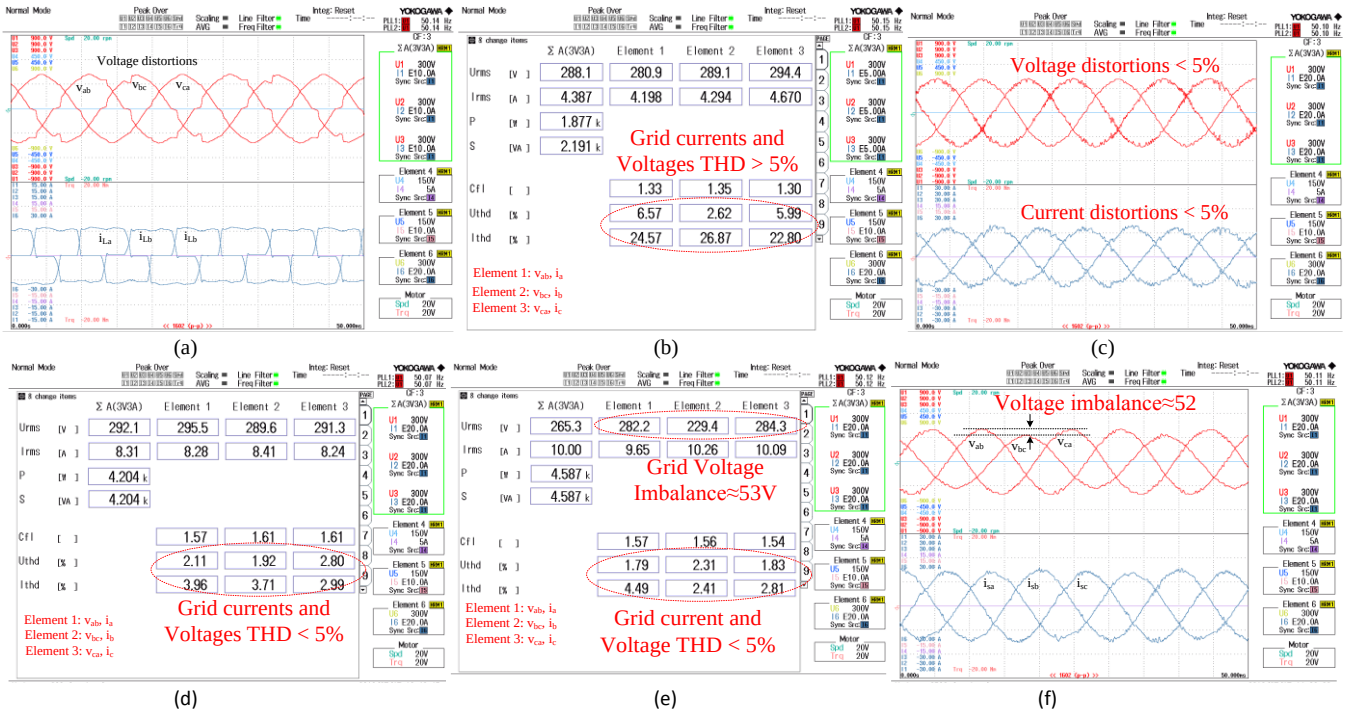

Fig. 9 (a-b). Performance of system under grid voltages distortion before switching on VSC, (c-d) Performance of system under grid voltages distortion after switching on VSC, (e) Magnitudes of system parameters under grid voltages imbalances condition and (f) Waveforms of grid voltages and currents under grid voltages imbalances condition

SPV coupled VSC supplies the compensating currents at PCC point. The grid currents are maintained well balanced and sinusoidal under weak grid condition. For the same reason, the grid power change from 1.877 kW to 4.204 kW has been noticed, however, the load power is the same. The THDs of grid voltages (v_{sab}, v_{sbc} and v_{sca}) are 2.11%, 1.92% and 2.80%. The THDs of grid currents (i_{sa}, i_{sb} and i_{sc}) are 3.96%, 3.71% and 2.99%. The THDs of the grid voltages and grid currents are achieved less than 5% according to IEEE-519 standard [25].

D. Dynamic Response of System at Grid Imbalance Condition

Figs. 9(e-f) depict the performance of the system under imbalance grid voltages. Fig. 9(e) depicts the RMS (Root Means Square) grid voltages (v_{sab}, v_{sbc}, v_{sca}) and it is noticeable imbalances in the grid voltages which is approximately 52 V between voltage 'v_{sbc}', 'v_{sab}' and 'v_{sca}'. Fig. 9(f) demonstrates the dynamics of grid voltages and currents under imbalanced grid voltages. Even though there is noticeable large imbalances in the grid voltages, it is observed from Figs. 9(e-f) that the grid currents (i_{sa}, i_{sb} and i_{sc}) are maintained balanced, sinusoidal and at unity power factor (UPF). Moreover, the THD of grid currents are within IEEE-519 standard limit. Solar PV system continues to supply power to the grid and connected loads.

E. Dynamic Response of System under Load Unbalancing

Figs. 10 (a-d) depict the response of the system under load unbalancing. Fig. 10 (a) demonstrates the dynamics of the DC link voltage (V_{DC}), grid, load and SPV coupled VSC currents of phase 'a' (i_{sa}, i_{la} and i_{vsc_a}). The DC link voltage is maintained stable under load unbalancing as shown in Fig. 10 (a). As unbalancing occurs in phase 'a' of load side network, power consumption of load is reduced, which results into an increase in power flow of the grid, as illustrated in Fig. 10 (a). The variation in SPV coupled VSC current in phase 'a' is shown in Fig. 10 (a). Fig. 10 (b) depicts the waveforms of grid voltage (v_{sab}), grid, load and SPV coupled VSC currents of phase 'b' (i_{sb}, i_{lb} and i_{vsc_b}). Fig. 10 (c) depicts the dynamics of the loss component (I_{loss}), PV feed-forward component (I_{pvff}), amplitude of the fundamental load component (I_{ap}), net weight of current component (I_{net}). The loss component (I_{loss}) remains unaltered under load unbalancing. The solar power generation under load unbalancing remains unaffected, which is demonstrated by dynamics of PV feed-forward component (I_{pvff}) as shown in Fig. 10 (a). The weight of fundamental load component is decreased to zero as unbalancing occurs in load side network of phase 'a'. The net weight of current component of reference grid current is negatively increased because the load power is decreased. Fig. 10 (d) shows the dynamic of the intermediate control signals of ISOGI-Q algorithm such as error (e(t)), quadrature and in-phase fundamental load component (i_{aqv}' and i_{av}'), unit template of phase 'a' (u_a). The in-phase and quadrature components decrease to zero as current in phase 'a' is reduced to zero. The unit template of phase 'a' remains unaffected even under load unbalancing.

F. Dynamic Response of System at Variable Solar Insolation

Figs. 10(e-f) show MPPT performance of solar PV emulator at two different solar insulations of 700 W/m^2 to 1000 W/m^2. The MPPT is observed perfectly well close to 100%. The dynamic performance of the system under solar insolation variation is depicted in Fig.11. As the solar insolation increases, the solar PV array current, solar power generation and consequ-

This article has been accepted for publication in a future issue of this journal, but has not been fully edited. Content may change prior to final publication. Citation information: DOI 10.1109/TIA.2017.2784374, IEEE Transactions on Industry Applications

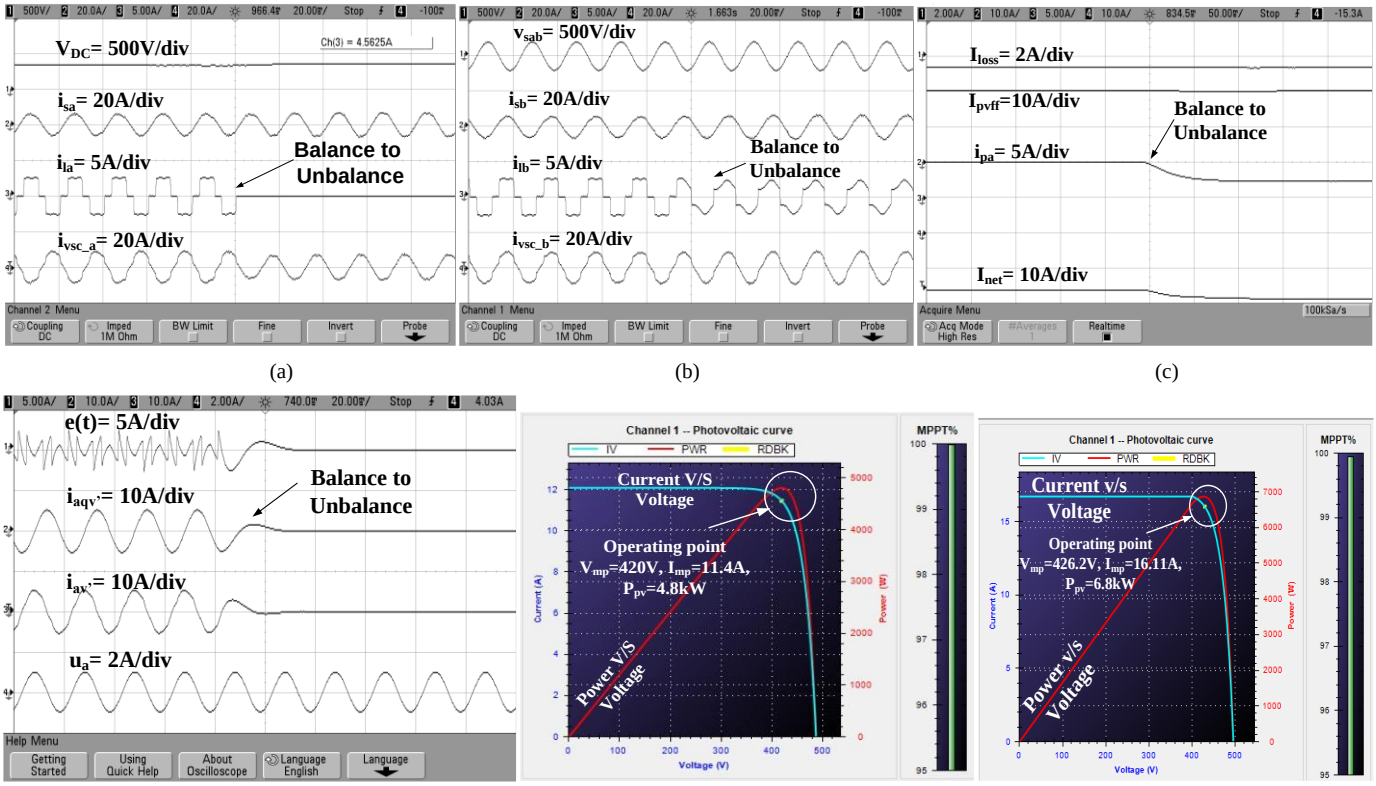

(a) (b) (c)

(d) (e) (f)

Fig. 10 Dynamic response of system under unbalancing (a) V_{DC}, i_{sa}, i_{la} and i_{vsc_a} (b) v_{sab}, i_{sb} ,i_{lb} and i_{vsc_b} (c) I_{loss}, I_{pvff}, i_{ap} and I_{net} (d) error, $i_{lqv'}$, $i_{lv'}$ and u_a , (e-f) MPPT performance of the solar PV array at 700W/m^2 and 1000W/m^2

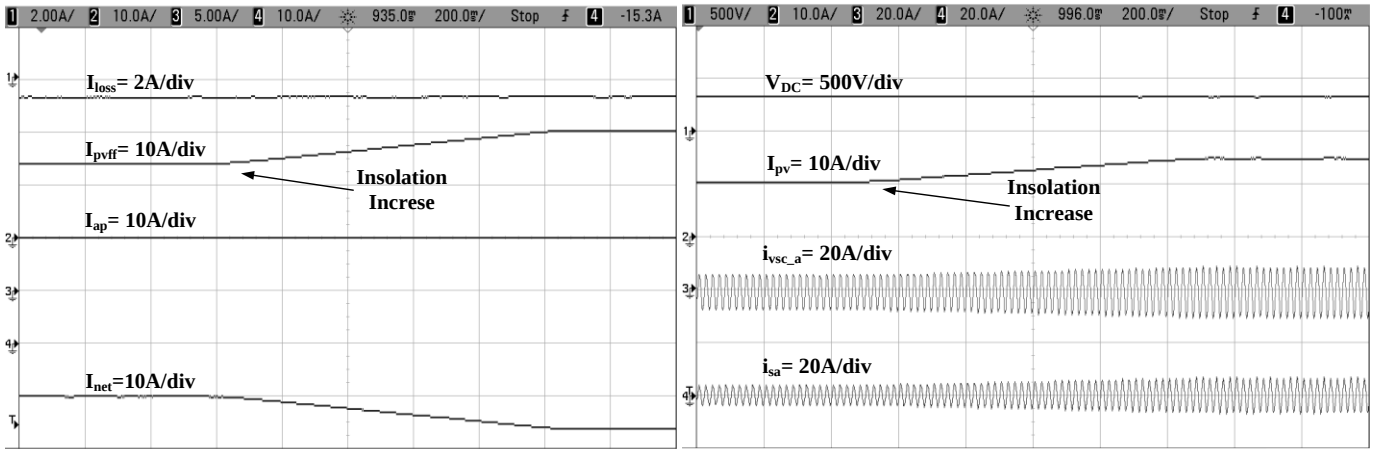

(a) (b)

Fig. 11 Response of system under variable solar insolation, (a) I_{loss}, I_{pvff}, I_{ap} and I_{net} (b) $V_{DC,}$ $I_{pv,}$ i_{vsc_a} and i_{sa}.

ently the grid current are increased. Fig. 11(a) shows intermediate signals such as the loss component (I_{loss}), PV feed-forward component (I_{pvff}), amplitude of fundamental component of load current (I_{ap}) and the net weight component (I_{net}). As PV feed-forward component is increased, net current component is increased as power consumption of the load remains unaffected. The amplitude extraction of fundamental load component is remains unaffected even under variation of solar power generation. The net weight of the current component is increased which results into an increment in amplitude of reference grid currents. Fig. 11(b) shows the dynamics of V_{DC}, SPV array current (I_{pv}), VSC current (i_{vsc_a}) and grid current (i_{sa}). The DC link voltage is maintained stable as shown in Fig. 11 (b). The power flow in the grid is increased, which is demonstrated by noticeable variation in the grid current and solar PV coupled VSC current.

V. Conclusion

An improved performance of a three phase single stage grid connected SPV based system has been demonstrated using ISOGI-Q based control algorithm to improve power quality of the distribution network such as unity power factor, harmonics mitigation and load balancing at distribution network. Frequency domain analysis demonstrates that proposed ISOGI-Q based structure has better DC offset filtering capability as

compared to conventional algorithms. The THD of grid currents are achieved within the limit of an IEEE-519 standard. Experimental results have shown that ISOGI-Q based control algorithm works satisfactory and robust during grid side and load side disturbances such as voltage imbalance, distorted grid voltages, variable solar insolation and load unbalancing.

APPENDICES

A. Simulation Parameters

Solar PV array details: PV array voltage, V_{mpp}= 710 V;PV array current, I_{mpp}=45A; PV array power, P_{pv}= 32.5 kW; grid voltage, v_{sab}= 415 V; DC bus voltage, V_{DC}= 710 V, DC bus capacitor, C_{dc}= 6mF; ripple filter: R_f= 5 Ω, C_f= 10 μF; L_f= 2.5 mH, k_{sq}=1.41; k_{DC}=0.22; T_s= 10 μs, nonlinear load= three phase diode bridge rectifier with R= 20 Ω, L= 80 mH.

B. Experimental parameters:

SPV array simulator, V_{mp}=421 V, I_{mp}=16.3 A, P_{pv}= 6.87 kW; DC link voltage= 421 V; converter rating= 25 kVA; ripple filter R_f =5 Ω, C_f =10 μF; Interfacing inductor L_f=2.9 mH; k_{sq}=1.41; k_{DC}=0.22; source voltage v_{sab} = 285 V, 50 Hz; non-linear load=1.85 kVA, linear load= 1.94 kVA; k_p=0.14, k_i=0.001; sampling time T_s= 30 μs.

ACKNOWLEDGMENTS

Authors are highly thankful to DST, Govt. of India, for supporting this project under Grant Number: RP02979.

REFERENCES

[1] L. Suganthi and A.Williams, "Renewable energy in India– a modeling study for 2020-2021"*Energy Policy*, vol. 28, no. 15,pp.1095-1109, 2000.

[2] A. Ashwin Kumar, "A study on renewable energy resources in India" in *Proc.International Conf. on Environmental Engineering and Applications*, pp.49-53, 10-12, 2010.

[3] M. G. Villalva, J. R. Gazoli and E. R. Filho, "Comprehensive approach to modeling and simulation of photovoltaic arrays" *IEEE Trans. Power Electronics*, vol.24, No. 5, May 2009.

[4] Anup Anurag, S. Bal, S. Sourav and M. Nanda, "A review of maximum power point tracking techniques for photovoltaic systems" *International Journal of Sustainable Energy*, vol.35, No. 5, 19 May 2014.

[5] M. E. El Telbany, A. Youssef and A. A. Zerky, "Intelligent techniques for MPPT control in photovoltaic systems: A comprehensive review" in *Proc.4th International Artificial Intelligence with Application Engineering and Technology*, pp.17-22, 3-5 Dec, 2014.

[6] Tsai-Fu Wu, Chih-Hao Chang, Li-Chuin Lin and Chia-Ling Kuo, "Power loss comparison of single and two stage grid-connected photovoltaic systems" *IEEE Trans. Energy Conversion*, vol. 26, no. 2, pp. 707-715, 2011.

[7] A. K. Barnes, J. C. Balda and C. M. Stewart, "Selection of converter topologies for distributed energy resources," in *Proc. IEEE Applied Pow. Electron. Conf. (APEC)*, pp. 1418-1423, 2012.

[8] R.N. Tripathi and A. Singh, "SRF theory based interconnected solar photovoltaic (SPV) system with improved power quality" in *Proc. IEEE Emerging Trends in Communication, Control, Signal Processing & Computing Application*, pp. 1-6, 10-11 Oct. 2013.

[9] D. Yazdani, A. Bakhshai and P. K. Jain, "A three-phase adaptive notch filter-based approach to harmonic/reactive current extraction and harmonic decomposition," *IEEE Transactions Power Electronics*, vol. 25, no. 4, pp. 914-923, April 2010.

[10] M. Qasim and V. Khadkikar, "Application of artificial neural networks for shunt active power filter control," *IEEE Transactions Industrial Informatics*, vol. 10, no. 3, pp. 1765-1774, Aug. 2014.

[11] H. Patel and V. Agarwal, "Investigations into the performance of photovoltaics-based active filter configurations and their control schemes under uniform and non-uniform radiation conditions," *IET Renewable Power Generation*, vol. 4, no. 1, pp. 12-22, January 2010.

[12] T. F. Wu, H. S. Nien, H. M. Hsieh and C. L. Shen, "PV power injection and active power filtering with amplitude-clamping and amplitude-scaling algorithms," *IEEE Transactions Industry Applications*, vol. 43, no. 3, pp. 731-741, May-june 2007.

[13] Nak-gueon Sung, Jae-deuk Lee, Bong-tae Kim, Minwon Park and In-keun Yu, "Novel concept of a PV power generation system adding the function of shunt active filter," in *Proc. IEEE/PES Transmission and Distribution Conference and Exhibition*, vol.3, pp. 1658-1663, 2002.

[14] C. Meza, D. Biel, D. Jeltsema and J. M. A. Scherpen, "Lyapunov-based control scheme for single-phase grid-connected PV central inverters," *IEEE Transactions Control Systems Technology*, vol. 20, no. 2, pp. 520-529, March 2012.

[15] M. Rezkallah, S. K. Sharma, A. Chandra, B. Singh and D. R. Rousse, "Lyapunov function and sliding mode control approach for the solar-PV grid interface system," *IEEE Transactions Industrial Electronics*, vol. 64, no. 1, pp. 785-795, 2017.

[16] I. M. B. Hassine, M. W. Naouar and N. Mrabet-Bellaaj, "Model predictive-sliding mode control for three-phase grid-connected converters," *IEEE Transactions Industrial Electronics*, vol. 64, no. 2, pp. 1341-1349, Feb. 2017.

[17] R. Agrawal, I. Hussain and Bhim Singh, "LMF based control algorithm for single stage three phase grid integrated solar PV system" *IEEE Trans. Sus. Energy*, vol. 7, no.4, pp.1379-1387, Oct 2016.

[18] S. Pradhan, I. Hussain, B. Singh and B. K. Panigrahi, "Modified VSS-LMS-based adaptive control for improving the performance of a single-stage PV-integrated grid system," *IET Science, Measurement & Technology*, vol. 11, no. 4, pp. 388-399, 7 2017.

[19] S. Vedantham, S. Kumar, B. Singh and S. Mishra, "Partially decoupled adaptive filter based multifunctional three phase GPV system," *IEEE Transactions Sustainable Energy*, Early Access.

[20] M. Ciobotaru, R. Teodorescu and V. G. Agelidis, "Offset rejection for PLL based synchronization in grid-connected converters," in *Proc. IEEE Applied Pow. Electron. Conference and Exposition*, pp. 1611-1617, 2008.

[21] B. Singh, P. Shah and I. Hussain, "ISOGI-Q based control algorithm for single stage grid tied SPV system," *2016 IEEE Uttar Pradesh Section International Conference on Electrical, Computer and Electronics Engineering (UPCON)*, Varanasi, pp. 501-507, 2016.

[22] H. K. Yada and M. S. R. Murthy, "A new topology and control strategy for extraction of reference current using single phase SOGI-PLL for three phase four-wire with shunt active power filter" in *Proc. IEEE Conf. Pow Electron., Drived Energy System (PEDES)*, pp. 1-6, Dec, 2014.

[23] C. Jain and B. Singh, "A SOGI-Q based control algorithm for multifunctional grid connected SECS" in *Proc. IEEE 6th India International Conf. Power Electronics (IICPE)*, pp. 1-6, 8-10 Dec. 2014.

[24] A. Luo, Y. Chen, Z. Shuai and C. Tu, "An improved reactive current detection and power control method for single-phase photovoltaic grid-connected DG system," *IEEE Transactions Energy Conversion*, vol. 28, no. 4, pp. 823-831, Dec. 2013.

[25] IEEE Recommended Practice and Requirement for Harmonic Control on Electric Power System, IEEE std. 519, 2014.

[26] B. Singh, A. Chandra and K. Al-Haddad, *Power quality: problems and mitigation techniques*, John Wiley & Sons Ltd., United Kingdom, 2015.

Bhim Singh (SM'99, F'10) was born in Rahamapur, Bijnor (UP), India, in 1956. He received his B.E. (Electrical) from University of Roorkee, India, in 1977 and his M.Tech. (Power Apparatus & Systems) and Ph.D. from Indian Institute of Technology Delhi, India, in 1979 and 1983, respectively.

In 1983, he joined the Department of Electrical Engineering, University of Roorkee (Now IIT Roorkee), as a Lecturer. He became a Reader there in 1988. In December 1990, he joined Department of Electrical Engineering, IIT Delhi, India, as an Assistant Professor, where he has become an Associate Professor

This article has been accepted for publication in a future issue of this journal, but has not been fully edited. Content may change prior to final publication. Citation information: DOI 10.1109/TIA.2017.2784374, IEEE Transactions on Industry Applications

in 1994 and a Professor in 1997. He has been ABB Chair Professor from September 2007 to September 2012. He has been Chair Professor from October 2012 to September 2017. He has been Head of the Department of Electrical Engineering at IIT Delhi from July 2014 to August 2016. Since, August 2016, he is the Dean, Academics at IIT Delhi. He is JC Bose Fellow of DST, Government of India since December 2015.

Prof. Singh has guided 68 Ph.D. Dissertations and 166 M.E./M.Tech./M.S.(R) theses. He has been filed 24 patents. He has executed more than eighty sponsored and consultancy projects. He has co-authored a text book on power quality: Power Quality Problems and Mitigation Techniques published by John Wiley & Sons Ltd. 2015.

His areas of interest include solar PV grid interfaced systems, microgrids, power quality monitoring and mitigation, solar PV water pumping systems, improved power quality AC-DC converters, power electronics, electrical machines, drives, renewable energy systems, FACTS, and high voltage direct current (HVDC) systems.

Prof. Singh is a Fellow of the Indian National Academy of Engineering (FNAE), The Indian National Science Academy (FNA), The National Academy of Science, India (FNASc), The Indian Academy of Sciences, India (FASc), The World Academy of Sciences (FTWAS), Institute of Electrical and Electronics Engineers (FIEEE), the Institute of Engineering and Technology (FIET), Institution of Engineers (India) (FIE), and Institution of Electronics and Telecommunication Engineers (FIETE) and a Life Member of the Indian Society for Technical Education (ISTE), System Society of India (SSI), and National Institution of Quality and Reliability (NIQR).

He has received Khosla Research Prize of University of Roorkee in the year 1991. He is recipient of JC Bose and Bimal K Bose awards of The Institution of Electronics and Telecommunication Engineers (IETE) for his contribution in the field of Power Electronics. He is also a recipient of Maharashtra State National Award of Indian Society for Technical Education (ISTE) in recognition of his outstanding research work in the area of Power Quality. He has received PES Delhi Chapter Outstanding Engineer Award for the year 2006. Professor Singh has received Khosla National Research Award of IIT Roorkee in the year 2013. He also received Shri Om Prakash Bhasin Award-2014 in the field of Engineering including Energy & Aerospace. He has received 2017 IEEE PES Nari Hingorani Custom Power Award.

He has been the General Chair of the 2006 IEEE International Conference on Power Electronics, Drives and Energy Systems (PEDES'2006), General Co-Chair of the 2010 IEEE International Conference on Power Electronics, Drives and Energy Systems (PEDES'2010), General Co-Chair of the 2015 IEEE International Conference (INDICON'2015), General Co-Chair of 2016 IEEE International Conference (ICPS'2016) held in New Delhi.

Priyank Shah (M'16) was born in Vadodara, Gujarat, India, in 1992. He received his B. E in Electrical Engineering from Birla Vishvakarma Mahavidyalaya (BVM), Gujarat, India, in 2013. He is currently pursing Ph. D degree in Indian Institute of Technology Delhi (IITD), New Delhi, India.

His areas of interest includes adaptive and learning control for renewable power generation, control techniques for intermittency mitigation, power system dynamics and power quality improvement of the distributed network and load frequency regulation.

Ikhlaq Hussain (M'14) was born in Doda, Jammu and Kashmir, India, in 1986. He received his B. E. (Electrical) from University of Jammu, Jammu, India, in 2009 and M. Tech. (Gold Medalist) in Electrical Power System Management from the Jamia Millia Islamia (A Central University), New Delhi, India, in 2012. He is currently working toward his Ph.D. in the Department of Electrical Engineering, Indian Institute of Technology Delhi, New Delhi, India.

From September 2012 to December 2012, he was a Lecturer with the Department of Electrical Engineering, National Institute of Technology Srinagar, India. On 19th April 2017, he joined as Assistant Professor in the Department of Electrical Engineering, Institute of Technology, University of Kashmir, Srinagar, India. His areas of research interests include power electronics, power quality, custom power devices, renewable energy systems, power system management and microgrid.

Mr. Hussain was a recipient of the POSOCO power system award (PPSA) from Power System Operation Corporation (POSOCO) Limited, India and Foundation for Innovation and Technology Transfer (FITT) at Indian Institute of Technology Delhi in 2017, and the IEEE INDICON Best Paper Award in 2015 and the IEEE UPCON Best Paper Award in 2016.